

## Role of the H bond and cooperative effects in normal and supercooled water studied by anisotropic low frequency light scattering

F. Aliotta, C. Vasi, G. Maisano, D. Majolino, F. Mallamace et al.

Citation: *J. Chem. Phys.* **84**, 4731 (1986); doi: 10.1063/1.450007

View online: <http://dx.doi.org/10.1063/1.450007>

View Table of Contents: <http://jcp.aip.org/resource/1/JCPSA6/v84/i9>

Published by the AIP Publishing LLC.

---

### Additional information on J. Chem. Phys.

Journal Homepage: <http://jcp.aip.org/>

Journal Information: [http://jcp.aip.org/about/about\\_the\\_journal](http://jcp.aip.org/about/about_the_journal)

Top downloads: [http://jcp.aip.org/features/most\\_downloaded](http://jcp.aip.org/features/most_downloaded)

Information for Authors: <http://jcp.aip.org/authors>

## ADVERTISEMENT

**physicstoday**

**Comment on any  
*Physics Today* article.**

**Measured energy in Japan**  
David von Seggern  
(vonneg@seismo.unr.edu) University of Nevada  
July 2012, page 10  
DIGITAL OBJECT IDENTIFIER  
<http://dx.doi.org/10.1063/PT.3.1619>  
The article by Thorne Lay and Hiroo Kanamori is an excellent review of the energy released by the 1994 Chilean earthquake. The authors estimate that the total strain energy release was approximately five times as much energy as that released by a 100-megaton atmospheric nuclear device. I believe the authors used the relation for seismic energy release rather than total strain energy release. The seismic energy release is a variable that depends on the fault plane. Accounting for total strain energy release would increase the earthquake energy number by orders of magnitude. Despite the catastrophic damage potential of nuclear bombs, the forces of nature occasionally unleash much larger energy releases. Although the nuclear bombs are under our control, earthquakes, volcanic eruptions, and extreme weather events are not. However, by judicious preparation and avoidance measures, humans can significantly diminish the damage of natural events. This article does not have any references.

**Comment on this article**  
By the act of hitting a ball with a bat, one calculates the force energy to deliver the ball to its new location, but one must also take into account that the ball extended its energy release to that which became struck by the ball as its momentum ceased and passed energy to the struck ball. Therefore the parameters of the damage extend into the future when the received energy to that pushed upon, later becomes released in a new event. Perhaps calculations of one added that in, while another's calculations did not. E.M.C.  
Written by Edgar McCarroll, 14 July 2012 19:59

# Role of the H bond and cooperative effects in normal and supercooled water studied by anisotropic low frequency light scattering

F. Aliotta and C. Vasi

*Istituto di Tecniche Spettroscopiche del CNR, Via dei Verdi, 98100 Messina, Italy*

G. Maisano, D. Majolino, F. Mallamace, and P. Migliardo

*Dipartimento di Fisica dell' Università, CISM and GNSM del CNR, Via dei Verdi, 98100 Messina, Italy*

(Received 22 April 1985; accepted 17 January 1986)

Depolarized Rayleigh and low frequency Raman scattering data in bulk supercooled water are presented. The measurements, performed from the normal region down to  $-26.95^{\circ}\text{C}$  for the first time, allow a quantitative data analysis and reveal the existence of a fine structure of the central contribution. We have identified a "fast" and "slow" contribution whose intensities show an opposite behavior as a function of temperature. Such a behavior is understood as a decay of local order due to the H bond. The spectral density function, as derived from the depolarized Raman data, shows the presence of acoustical and intermolecular optical contributions characteristic of many structured disordered materials. A critical comparison with molecular dynamics (MD) and neutron scattering results is also presented.

## I. GENERAL CONSIDERATIONS

Very recently the diffusional and vibrational dynamics of liquid water, especially in the supercooled region, have been investigated with a variety of techniques.<sup>1-7</sup> New theoretical models<sup>8-11</sup> and molecular dynamics calculations<sup>12-15</sup> have recently been developed for better understanding of the structural and dynamical properties of such a system, especially as far as the role of the intermolecular bonds is concerned. It is rather commonly accepted that the existence of the hydrogen bond and its highly directional intermolecular potential  $V(r)$ <sup>1,13,16,17</sup> is the main reason of the peculiar properties of water. It is well known that many of the physical quantities (specific heat, thermal expansivity, isothermal compressibility, etc.) show an unusual temperature dependence in the metastable supercooled region<sup>1,2</sup> where the H bonds play a fundamental role in determining the dynamical and static properties of the system. In fact, the strong directional hydrogen bond in  $\text{H}_2\text{O}$  gives rise to a local tetrahedral<sup>18,19</sup> arrangement with a three-dimensional connectivity that increases as the temperature is lowered.

In order to explain this fact, various theoretical models<sup>20</sup> have been proposed, historically divided into continuous and discrete ones, both having in common the fact that a local four-coordinated environment with low density is preferred for the structural arrangement. Recently,<sup>14</sup> MD results on supercooled water seemed to overcome the question if the bond connectivity of the system looks like a continuous polymeric network or, in terms of a site-connectivity language, it looks like an ensemble of low density patches. As a matter of fact, because the H bond is the origin of the intermolecular connectivity and because the mean lifetime lies in the ps time scale, water could be seen as a "locally structured transient gel"<sup>14</sup> in which the structure evolves in time through a continuous breaking and making of bonds. This circumstance together with the possible existence of

many bonds (up to four) for the molecules with varying strength and symmetry, gives rise to a variety of "inherent structures"<sup>8</sup> corresponding to a local minima in the potential energy for the system. Recently Stillinger and Weber<sup>8</sup> calculated the set of such inherent structures. These authors, also on the basis of MD results, explained the water anomalies at low temperature as due to the growing of some relevant inherent structure (tetrahedral) as the temperature decreases. The "critical" singularity<sup>1</sup> at the supercooling limit might be due to some super arrangement of the tetrahedral units into hydrogen bond polyhedra with an extent from 10 to 30 Å. Furthermore, as in the case of five water molecules that develop a complete hydrogen bond network<sup>13</sup> by arranging themselves in a tetrahedral unit, then the only way for an extended network of tetrahedral units to exist in the deeply supercooled region (no crystallites) is their organization in random oriented polyhedra with pentagonal<sup>8,21</sup> faces. This structure is also topologically favorable and tends to be "autocatalytic" (i.e., the probability for the existence of a polyhedron increases near a preexisting one). As will be explained, the H-bond properties (lifetime, breaking time, energy, etc.), together with the existence of such transient gel, are deeply connected with the anisotropic contribution to the light scattering by supercooled water.

The present work is a part of an extensive study that our group carried out on supercooled water by spectroscopic methods.<sup>4,22,23</sup> We have previously measured hypersonic velocity and absorption in bulk water down to  $-27^{\circ}\text{C}$  by means of Brillouin scattering, and the results showed that the high frequency sound velocity has a well defined minimum at about  $-22^{\circ}\text{C}$ , with a simultaneous flattening in the acoustical absorption. This implies the existence of a structural and/or a viscous relaxation phenomenon, strength, and relaxation times have been evaluated by us. Furthermore, the analysis of the temperature evolution of the iso-

tropic part of the spectrum, measured down to  $-25.5^\circ\text{C}$ , has allowed a precise determination of the Landau–Placzek ratio (LPR).<sup>23</sup> This important physical quantity, for the first time evaluated in the supercooled region, exhibits a large temperature variation which has been explained on the basis of the existence of a structural relaxation process involving the “more structured” part of water. In this work we report a detailed analysis of the low frequency depolarized light scattering  $I_{\text{VH}}(\omega)$  as a function of temperature both in the normal and in the supercooled liquid phase down to  $-26.95^\circ\text{C}$ . We will show that the spectrum exhibits a fine structure in the central contribution, whose linewidth and intensity evolution as a function of temperature reflects the structural anisotropy induced by the strong intermolecular H bond. In addition we will show that the optical contributions also exist at frequencies lower than  $300\text{ cm}^{-1}$ , and are characterized by broad depolarized components connected with the hindered translational motion of the tetrahedral cage. These broad components closely resemble the features shown by the generalized frequency distribution obtained by MD calculations<sup>15</sup> and by incoherent inelastic neutron scattering measurements.<sup>24,25</sup>

## II. EXPERIMENTAL SETUP, PROCEDURE, AND HANDLING OF DATA

The depolarized light scattering measurements were performed on a 10 cc vial containing very high purity, doubly distilled, deionized, and dust-free water, purchased from the Angelini pharmaceutical industry. The relatively large size of the sample, together with the use of an optical thermostat especially built to avoid any unwanted stray-light effects, allowed us to collect data with good signal-to-noise ratio and without spurious effects. During the measurements the temperature was held constant within  $0.02^\circ\text{C}$ . We used a  $90^\circ$  scattering geometry with a high resolution fully computerized Spex triple monochromator using the  $4880\text{ \AA}$  line of a spectra physics unimode  $\text{Ar}^+$  laser as the exciting source whose exciting mean power was 1 W. The entire experimental setup, as well as the collection and normalization of the data, was controlled on line by Digital Minc 11/23 minicomputer. As mentioned in Sec. I, the present work is devoted to a careful analysis of the  $I_{\text{VH}}(\omega)$  contributions to the spectra in the low frequencies region.

Due to the low efficiency of the depolarized scattering of water, in order to obtain a good signal-to-noise ratio in the  $-20$  to  $+20\text{ cm}^{-1}$  region, we have used a spectral resolution of  $0.045 \pm 0.004\text{ cm}^{-1}$  (HWHM) in the  $-1$  to  $+1\text{ cm}^{-1}$  region, of  $0.2\text{ cm}^{-1}$  in the  $-5$  to  $+5\text{ cm}^{-1}$  region and of  $0.5\text{ cm}^{-1}$  in the  $-20$  to  $+20\text{ cm}^{-1}$  region. In the region  $20$ – $700\text{ cm}^{-1}$ , a resolution of  $2\text{ cm}^{-1}$  was used. As an example, in Fig. 1 we show a typical  $I_{\text{VH}}$  spectrum, taken at  $3.77^\circ\text{C}$ , in the spectral range from  $-12$  to  $+12\text{ cm}^{-1}$ . The three spectra at different resolutions were numerically matched, normalized for the incident beam intensity, corrected for the density  $\rho$  and the refractive index  $n$ , and finally, corrected for local field effects.<sup>22,26</sup> The last two corrections are taken into account through the factor  $n\rho^{-1} \cdot (n^2 + 2)^{-4}$ , where the  $n$  and  $\rho$  are taken from literature (see Ref. 4 for details). The maximum resolution ob-

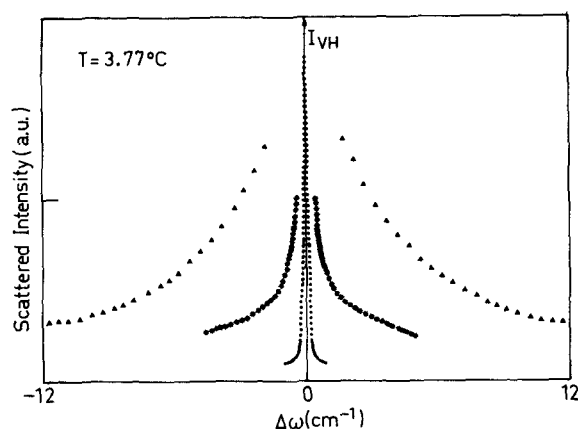


FIG. 1. Depolarized Rayleigh wing spectrum at  $T = +3.77^\circ\text{C}$ . Dots, stars, and triangles refer to  $0.045$ ,  $0.2$ , and  $0.5\text{ cm}^{-1}$  band pass, respectively. (See the text for details.)

tainable from our spectrometer in the  $-1$  to  $+1\text{ cm}^{-1}$  region was initially carefully checked by recording the spectrum from an aqueous latex suspension.

## III. ANALYSIS OF THE DEPOLARIZED SCATTERING MECHANISM AND EXPERIMENTAL RESULTS

It is well known that the nonshifted depolarized light scattering is caused by the fluctuation of the traceless part of the polarizability tensor.<sup>27</sup> The corresponding time correlation function  $C_{\beta}^{\text{Anis}}(t)$  and its Fourier transform  $I_{\text{VH}}(\omega)$  can be characterized by various contributions, which depend on the different mechanisms involved in the scattering processes.

Usually the Rayleigh wing is written in the form

$$I_{\text{VH}}(\mathbf{k}, \omega) = \int_{-\infty}^{\infty} dt e^{-i\omega t} \cdot \{ \langle \delta\alpha_{xy}^*(\mathbf{k}, 0) \delta\alpha_{xy}(\mathbf{k}, t) \rangle \cdot \sin^2 \theta / 2 + \langle \delta\alpha_{yz}^*(\mathbf{k}, 0) \delta\alpha_{yz}(\mathbf{k}, t) \rangle \cos^2 \theta / 2 \}. \quad (1)$$

In Eq. (1),  $\langle \rangle$  denotes the thermodynamic averaging,  $\delta\alpha_{ij}(\mathbf{k}, t)$  indicates the traceless part of the polarizability fluctuation tensor,  $\theta$  is the scattering angle, and the scattering geometry is the same as that described in Ref. 27. The terms  $\delta\alpha_{ij}$  also take into account the translational contribution. For low viscous liquids with weak intermolecular interactions under the assumption that coupling between rotational motion and collective hydrodynamic transport modes can be neglected, the Rayleigh wing contains mainly two contributions: (i) the far wing ( $\omega \gtrsim 30\text{ cm}^{-1}$ ), due to collisional interactions, and (ii) the narrow wing ( $\omega \lesssim 30\text{ cm}^{-1}$ ) caused by the molecular rotational motion.<sup>28,29</sup>

The depolarized central contribution (narrow wing) consists of a sum of the single particle term, similar to the depolarized component of the Raman vibrational lines, and of a pair term related to the cooperative reorientational relaxation processes.<sup>27,30</sup> In this respect, the light scattering response is different from the incoherent quasielastic neutron scattering response<sup>31,32</sup> which probes “only” single molecules reorientational relaxation rate processes.

Keyes and Kivelson were able to unify the various mod-

els for the reorientational relaxation processes as seen by light scattering experiments, by introducing the “pseudo-GLED-SLOR” theory<sup>33</sup> based on Mori’s formalism for the generalized hydrodynamics. This theory can be applied to “structure limited” or “associated” liquids (e.g., H-bonded liquids,<sup>30,34</sup> molecular liquids,<sup>35,36</sup> molten salts,<sup>37</sup> and electrolytic solutions<sup>24</sup>). For these systems the molecules (or ions) are half fixed until structural breakup occurs; before such a breakup the molecules undergo a librational motion in a potential well due to the first neighbor interactions. Then, for time intervals sufficiently small, one can define an equilibrium orientational direction. At longer times, as the local structure is expected to randomize or melt, the molecule may freely reorient itself to a new angular position. Within the framework of such a theory in the SLOR limit, we can define  $\tau_{\text{RES}}$  as the time during which a molecule remains trapped into an appropriate torsional well. Then the depolarized spectrum will consist of a central Lorentzian line plus a torsional Raman line centered at high frequencies. This picture is appropriate to our case so that it seems that the SLOR approximation should hold for supercooled water. In particular the  $I_{\text{VH}}(\omega)$  in the above approximation will show a weak high frequency librational shoulder, a symmetrical central contribution (fast Lorentzian) that will be related to the dynamical evolution of the local structure, and a slow Lorentzian that will be connected to the exponential decay of the orientational correlation function. As far as the orientational dynamics in liquid water are concerned, many experiments performed both in the normal<sup>28,29,38</sup> and in the supercooled region,<sup>39,40</sup> have put in evidence a fast central contribution, connected to the existence of a local structure. Furthermore a slow contribution<sup>28,39</sup> exists, whose intensity seems to increase as the temperature decreases and it is assigned to the reorientation of the water molecules. The presence of this latter contribution seems to have a peculiar importance, mainly because it gives the possibility of a direct comparison with neutron measurement of  $\tau_{\text{OR}}$  in normal<sup>5,38</sup> and in supercooled water.<sup>5</sup> Finally, the additional presence of a weak librational shoulder, in the range from 500–700  $\text{cm}^{-1}$ , whose intensity increases by lowering  $T$ , supports the idea that one of the SLOR models is applicable to the water. However the static anisotropic polarizability  $\langle \beta_0 \rangle$  is very weak, the  $\text{H}_2\text{O}$  molecule being roughly spherical, moreover the number of unbonded molecules is very low (for instance, at  $T \simeq +10^\circ\text{C}$  the percentage of monomers is less than 1%) so that the scattered intensity corresponding to this process should be much smaller than reported in the literature. Under these circumstances we think that experimental depolarized central line has a different physical origin. The situation seems to be very similar to the one discovered for alcohols by Fytas and Dorfmueller,<sup>34</sup> who detected a slow contribution to  $I_{\text{VH}}(\omega)$  (mainly induced by the H-bonded intermolecular structure), whose intensity increases when the temperature decreases. Another peculiarity of liquid water is the presence of viscoelastic effect,<sup>4</sup> that results in a  $\omega$  dependence of the transport coefficients. As stressed above, for temperatures lower than  $-15^\circ\text{C}$ , both the shear and the bulk viscosity relax as a function of frequency. This implies a non-Newtonian behavior, with the possibility that transverse phenom-

ena<sup>27,41,42</sup> take place in the system. These phenomena should play a role in determining the fine structure of the central line.

All the abovementioned circumstances imply that, in water, the  $I_{\text{VH}}$  spectrum may be mainly connected with the relaxation time of the local order extending for small distances, but not negligible in comparison with the inverse of the exchanged wave vector of the probe. Because of the presence of a hierarchy in the structure (tetrahedral units, extended polyhedron, etc.) with a spatial extension that increases when  $T$  decreases, one must expect the anisotropic contribution to arise from the decay of the correlations of these local order fluctuations.<sup>42</sup> Furthermore there exists the possibility of an appearance of spectral contributions, due to viscoelastic effects, that arise from some coupling of translational local order with the transport parameters. This coupling could cause, for example, the appearance of a Rytov dip.<sup>27</sup> We have estimated that in the case of water at  $T = -25^\circ\text{C}$  the Rytov dip width  $\gamma = K^2 \cdot \eta_s / \rho$  is about 2 GHz.

In summary, on the basis of the arguments discussed above and by considering all the processes that take place, the total depolarized low frequency scattering intensity will be given by

$$I_{\text{Anis}}^{\text{Total}}(\omega) = S(\omega) + \mathcal{L}_{\text{LO}}^{\text{slow}}(\omega) + \mathcal{L}_{\text{LO}}^{\text{fast}}(\omega) + I_{\text{Anis}}^{\text{Vibr}}(\omega). \quad (2)$$

In Eq. (2),  $S(\omega)$  represents an “ultranarrow” symmetric contribution, resolution enlarged, which can be originated by the translational diffusional mechanism and could be convoluted, in the lower temperature limit, with possible “transverse” spectral contributions. The  $\mathcal{L}_{\text{LO}}^{\text{fast}}(\omega)$  and  $\mathcal{L}_{\text{LO}}^{\text{slow}}(\omega)$  Lorentzian lines are related to the exponential time decay of the local order through a fast and a slow process, this latter becoming predominant in the supercooled region. Each Lorentzian line furnishes two important parameters: the HWHM  $\Gamma = (2\pi\tau)^{-1}$ , and the integrated area, related with the static mean anisotropic polarizability of the implied structure. The  $I_{\text{Anis}}^{\text{Vibr}}(\omega)$  is the low frequency contribution of the vibrational spectral density  $g(\omega)$ . In general, this cooperative contribution is written in the form<sup>24,36</sup>

$$I_{\text{Anis}}^{\text{Vibr}}(\omega) = (\omega_0 - \omega)^4 \cdot \frac{[n(\omega, T) + 1]}{\omega} \cdot P(\omega) \cdot g(\omega), \quad (3)$$

where  $P(\omega) \cdot g(\omega)$  is the effective Raman vibrational density of states  $g_{\text{eff}}^{\text{R}}(\omega)$ ,  $P(\omega)$  being a Raman mode and frequency dependent electron–vibration coupling function. In the region from 0–20  $\text{cm}^{-1}$  both the quasielastic and the  $I_{\text{Anis}}^{\text{Vibr}}(\omega)$  terms are present. The latter behaves like an essentially constant background and hence we have fitted every spectrum, after the normalization procedure described in Sec. II, with two Lorentzians convoluted with a Voigt function plus a constant background. The result of the least square fit, together with the experimental spectra, are shown in Fig. 2 for three temperatures in the spectral region from  $-20$  to  $+20^\circ\text{C}$ .

Finally knowing the values of the integrated intensity and the linewidth for the Lorentzians, we have removed the quasielastic contribution from the spectra by subtracting it

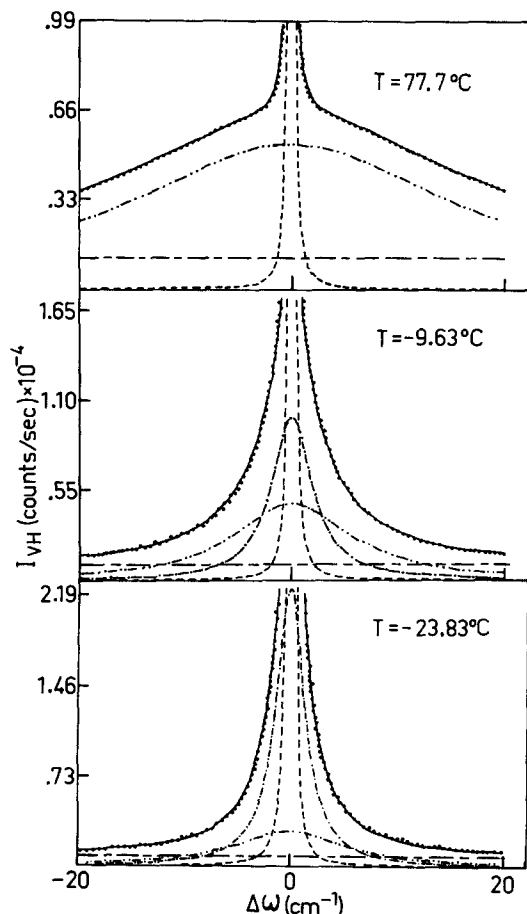


FIG. 2. Temperature evolution of depolarized Rayleigh wing. The full curves through the experimental points (dots) are the results of a fit using two Lorentzians convoluted with a Voigt function plus a constant background. --- Voigt profile; -.- fast Lorentzian contribution; ..... slow Lorentzian contribution; --- constant background.

from the experimental  $I_{\text{Anis}}^{\text{Total}}(\omega)$  and we have thus obtained  $g_{\text{eff}}^R(\omega)$ , starting from the very low frequency region up to  $300 \text{ cm}^{-1}$  of the Stokes shift.

#### IV. DISCUSSION

##### A. Local order diffusional dynamics: Fast contribution

In Fig. 3 we show the behavior of the integrated intensity of the fast and slow Lorentzians, obtained by our fitting. In Figs. 4 and 5 we represent the  $T$  dependence of the relaxation time  $\tau^{\text{fast}}$  and of the integrated intensity  $I_{\text{VH}}^{\text{fast}}$  obtained

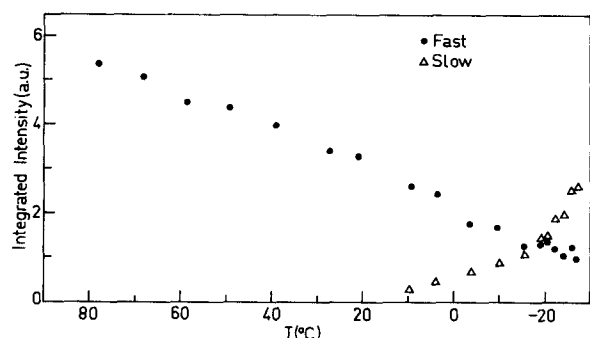


FIG. 3. Plot of the integrated intensity vs  $T$  for the fast and slow contribution.

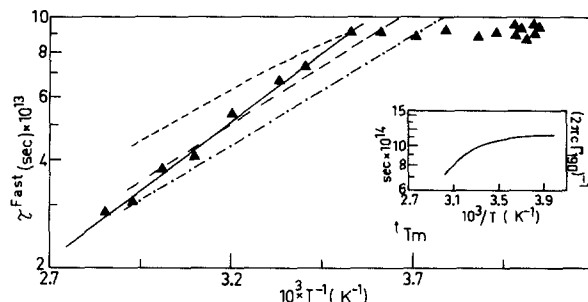


FIG. 4. Arrhenius plot of the fast relaxation time.  $\blacktriangle$ : this work. —: theoretical fit. ---: Ref. 29; -.-: Ref. 39; .....: Ref. 28. In the inset the behavior of the inverse  $190 \text{ cm}^{-1}$  linewidth vs  $T^{-1}$  (Ref. 6) is shown.

from the fitting of the experimental spectra.

As it can be noticed the integrated intensity increases with increasing temperature. This fact implies that the mean optical molecular anisotropy connected with this fast process lowers when  $T$  decreases. In addition, the relaxation time of the fast decay of the local order shows an Arrhenius behavior in the temperature range  $+80$  to  $+10^\circ\text{C}$  and an almost constant value in the range  $+10$  to  $-26.95^\circ\text{C}$ . This implies that there are two regimes for the system: the first one is peculiar to the normal liquid region and the second is characteristic of the supercooled region. For liquids like water<sup>28</sup> and alcohols,<sup>34</sup> the presence of this fast central contribution is connected to the dynamics of the hydrogen bond. If in the first region (i.e.,  $T > 10^\circ\text{C}$ ) the values of  $\tau^{\text{fast}}$  are plotted vs the corresponding reciprocal absolute temperature, a straight line is obtained: this fact suggests the existence of a thermally activated relaxation process. By applying a crude two-state model, we assume that every molecule could exhibit an intact (state on) or broken (state off) bond. This is analogous to the "bond-lattice" model,<sup>43</sup> that has been successfully applied to investigate the properties of associated liquids. The transition from one state to the other one is considered to be a thermally activated process (i.e., it takes place through a potential barrier  $\Delta G^\ddagger$ ). The existence of two possible states for the molecules implies that the anisotropic polarizability tensor changes depending on the level of occupancy of the two states, and its correlation function decays exponentially with time. As a consequence whereas the  $\tau^{\text{fast}}$  will contain information about the activation energy, the in-

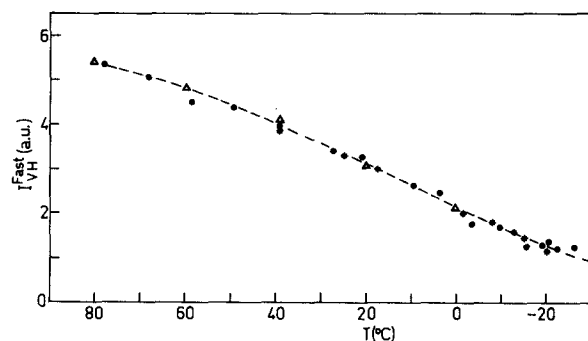


FIG. 5. Plot of the fast Lorentzian area vs  $T$ . Dots: this work. Triangles: complementary intensity of the librational band Ref. 46. Stars: complementary intensity of the bond stretching band (Ref. 6). Dashed line: theoretical fit. (See the text.)

egrated intensity will give information about the binding energy. If  $n_1$  and  $n_2$  are the numbers of “intact” and “broken” bonds in the scattering volume of the sample, then the kinetic equation

$$n_1(t) \xrightleftharpoons[k_2]{k_1} n_2(t)$$

can describe the chemical equilibrium between the on and off states.

Following the same procedure that was successfully applied to the Rayleigh wing analysis of molten  $\text{SbCl}_3$ ,<sup>36</sup> we can state that fluctuations of  $n_1(t)$  around the equilibrium value decay exponentially in time, with a time constant  $\tau = (k_1 + k_2)^{-1}$ , whereas the “magnitude” of the fluctuations is given<sup>44</sup> by

$$\bar{n}_1^2 - (\bar{n}_1)^2 = \bar{n}_2^2 - (\bar{n}_2)^2 = \frac{n_1^0 \cdot n_2^0}{n} \propto P_B \cdot (1 - P_B) \quad (4)$$

with

$$P_B = \frac{n_1^0}{(n_1^0 + n_2^0)} = \left[ 1 + \exp\left(-\frac{\Delta G}{RT}\right) \right]^{-1},$$

$P_B$  being the probability of finding a bond in the on state and  $\Delta G = \Delta H - T\Delta S + P\Delta V$ . Therefore, the integrated intensity  $I_{\text{VH}}^{\text{fast}}$ , connected with  $\bar{n}_1^2 - (\bar{n}_1)^2$  gives information about the binding energy value  $\Delta G$ . The fitting of the experimental data with the Eq. (4) furnishes a value of the binding enthalpy  $\Delta H = 6730 \text{ cal mol}^{-1}$  for the process. As far as the time constant  $\tau^{\text{fast}}$  is concerned, the Arrhenius fit of the data gives an activation energy value of  $3400 \text{ cal mol}^{-1}$ . Furthermore it is to be expected that the breaking of the two bonds of a central  $\text{H}_2\text{O}$  molecule, in the tetrahedral environment, causes the decreasing of the intensity for both the librational band (that lies in the  $450\text{--}780 \text{ cm}^{-1}$  spectral range) and the translational band,<sup>45,46</sup> and also produces a corresponding increase in the central component due to the activation of the anisotropic contribution. The temperature variation of the complementary intensity of the torsional band and of the bond stretching band<sup>6</sup> agree very well with the behavior of our data when normalized at the same temperature.

As far as the fast spectral contribution in the supercooled phase is concerned, because the overall structure tends to a larger spatial extension, different microscopic dynamic processes can take place. The behavior of the  $\tau^{\text{fast}}$  vs  $T$  clearly indicates that the fast relaxation time becomes temperature independent in the range from  $+10$  to  $-26.95^\circ\text{C}$ . This is similar to the behavior recently observed for the temperature evolution of a depolarized central component in ice Ih by Signorelli and co-workers.<sup>47</sup> These authors discovered a Rayleigh wing contribution (Lorentzian) whose width was connected to the frequency of creation and annihilation of Bjerrum and ionization defects. The value of  $\tau$  ( $\approx 1 \text{ ps}$ ) obtained was almost temperature independent, indicating that the activation energy for this process is much lower than  $K_B T$  in the investigated ( $185\text{--}270 \text{ K}$ ) range of temperature; at the same time the integrated area (intensity) decreases with increasing temperature. Thus, a “defect diffusion” model (e.g., the Glarum model) can hold in supercooled water as well. In this model the cooperative molecular reorientation motion is triggered by the free volume in the liquid,

which is related to the presence of a defect or of a vacancy in the immediate neighborhood of a molecule trapped in the structural network. If one assumes that these vacancies (or defects) move through the liquid, a breaking of bonds arises with a subsequent reorientational motion of the molecule close to the defect. Furthermore, if the activation energy of this process is lower than  $K_B T$ ,  $\tau^{\text{fast}}$  will be temperature independent.

In our case,  $\tau^{\text{fast}}$  in the supercooled region is independent of  $T$  and its value of  $0.9 \text{ ps}$  is very close to the one obtained for the ice. Finally, as shown in the inset of Fig. 4, the inverse of the  $190 \text{ cm}^{-1}$  band linewidth<sup>6</sup> shows a behavior vs  $T$  similar to the one we found in the supercooled region. This flattening effect was explained by the authors as the tendency of the local structure of water to evolve towards a limiting structure (vitreous ice).

## B. Local order diffusional dynamics: Slow contribution

The Rayleigh wing component connected with the slow time decay of the local order, namely  $\mathcal{L}_{\text{LO}}^{\text{slow}}(\omega)$ , shows a temperature dependence. In particular  $\tau^{\text{slow}} = (2\pi c \Gamma^{\text{slow}})^{-1}$  is a decreasing function of the temperature (Fig. 6). By fitting the experimental data in the range  $10$  to  $-26.95^\circ\text{C}$ , with the Arrhenius law

$$\tau^{\text{slow}} \cdot T = (\tau^{\text{slow}} \cdot T)_0 \cdot \exp(\Delta H/RT)$$

we have obtained an activation enthalpy of  $2380 \text{ cal mol}^{-1}$ . In Fig. 6, the neutron reorientational relaxation times  $\tau_{\text{OR}}^{\text{N}} \cdot 5$  are showed, for comparison. As expected, our  $\tau^{\text{slow}}$  values are higher than  $\tau_{\text{OR}}^{\text{N}}$ , indicating that other contributions than the single molecule reorientational motion are present. On the other hand, the corresponding values of the integrated intensity  $I_{\text{VH}}^{\text{slow}}$  (triangles in Fig. 3), that characterize the slowly varying optical anisotropy of the intermolecular H bond aggregates, show a marked increase when the temperature is lowered down to  $-26.95^\circ\text{C}$ . This intensity can be directly connected with the long time tails of the correlated fluctuations of the local order of water. In particular,<sup>34</sup> the VH intensity can be written in the following form:

$$I_{\text{VH}}^{\text{slow}} = N^* \cdot \langle \beta^* \rangle^2, \quad (5)$$

where  $N^* = N_{\text{bond}}/N_{\text{Total}}$  represents the concentration of that H bonded molecules in the scattering volume with a mean optical anisotropy  $\langle \beta^* \rangle$ . The values of  $I_{\text{VH}}^{\text{slow}}$  show a complicated temperature dependence which could be due to the fact that for each temperature a different extended struc-

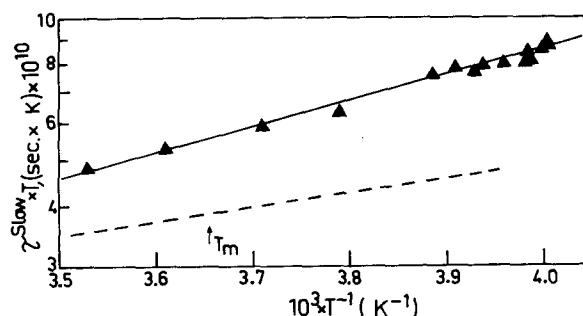


FIG. 6. Arrhenius plot of the slow relaxation time.  $\blacktriangle$ : this work. —: theoretical fit. - - -:  $\tau_{\text{OR}}^{\text{N}}$  from Ref. 5.

tural aggregate exists, each one with different  $N^*$  and  $\langle \beta^* \rangle$  values. However a definite physical interpretation of our data is difficult to make in view of the part that nothing is known about the  $T$  dependence of  $N^*$  and  $\langle \beta^* \rangle$ . Anyway, it is worthwhile to stress some relevant results we obtained:

(a) the  $I_{\text{VH}}^{\text{slow}}$  intensity, is appreciably different from zero only for  $T \lesssim 10^\circ\text{C}$ , becoming predominant in the deeply supercooled phase, with an over increased temperature derivative.

(b) The slow process, as in the case of the fast contribution, is thermally activated, with an enthalpy value very similar to that of the fast process. This implies that the H-bond dynamics play a role in spectral nonshifted contributions. Furthermore, as can be seen in Fig. 3, the  $I_{\text{VH}}^{\text{slow}}$  shows an almost-linear dependence on the temperature in the region from  $+10$  to  $-10^\circ\text{C}$ . On the basis of arguments similar to those appearing in Ref. 34, it is possible to postulate [see Eq. (5)] that the main contributing  $N^*$  is related only to one kind of structural environment with an appropriate static anisotropy. By decreasing the temperature, the slope of  $I_{\text{VH}}^{\text{slow}}$  vs  $T$  increases, indicating that different contributions to the optical anisotropy take place, in which both  $N^*$  and  $\langle \beta^* \rangle$  are  $T$  dependent. If  $\langle \beta^* \rangle$  was temperature independent, the  $dI_{\text{VH}}^{\text{slow}}/dT$  values would be directly connected with  $dN^*/dT$ . In this case, the behavior of  $dI_{\text{VH}}^{\text{slow}}/dT$  could be compared with experimental and theoretical determination of  $dN^*/dT$ . In Fig. 7 we represent some of these quantities related to the existence of a more structured part of water. In particular: curve (a) is the derivative of the concentration of the intact H bond  $dn_x/dT$ <sup>43</sup>; curve (b) represents the derivative

of the concentration of four-bonded molecules  $df_4/dT$ <sup>48</sup>; curve (c) represents the derivative of the concentration of the pentagonal units  $dN_5/dT$ <sup>21</sup>; curve (d) represents the measured values of  $dI_{\text{VH}}^{\text{slow}}/dT$ . The open circles represent the temperature derivative of the number density  $(\partial\rho_1/\partial T)_P$  of the structured water molecules that contribute to the dielectric constant and to the Landau-Placzek ratio variations in the supercooled water.<sup>23</sup> From an inspection of Fig. 7, it is possible to notice that the more "complex" the structure, the more rapidly the temperature derivative increases when  $T$  decreases. In particular, our  $dI_{\text{VH}}^{\text{slow}}/dT$  agrees very well with the behavior of  $(\partial\rho_1/\partial T)_P$  down to  $-15^\circ\text{C}$ . This circumstance indicates that the mean polarizability  $A_1$  of the more structured water, and its anisotropic mean component  $\langle \beta^* \rangle$  contributes to both processes. Finally, for temperature lower than  $-15^\circ\text{C}$ , the  $dI_{\text{VH}}^{\text{slow}}/dT$  shows a sharper increase than  $(\partial\rho_1/\partial T)_P$ . This seems to indicate that at lower temperatures, where a more extended H-bonding network is expected, interaction effects between the various polyhedra give rise to a  $T$  dependence of  $\langle \beta^* \rangle$ .

### C. Low frequency H-bond induced vibrational dynamics

Following the procedure explained in Sec. III, we have obtained the effective Raman density of states  $g_{\text{eff}}^R(\omega)$  and the reduced  $I^R(\omega) = g_{\text{eff}}^R(\omega)/\omega$ , as a function of temperature. In Figs. 8 and 9, the spectral distribution functions are shown for two temperatures, in the region from  $0$ – $300\text{ cm}^{-1}$  of Stokes shift. The most important features in the spectra are two broadbands centered at about  $60$  and  $190\text{ cm}^{-1}$  plus a low frequency contribution. This low contribution closely resembles the spectral distribution of many amorphous solids<sup>49</sup> and many structured liquids.<sup>36</sup> We have interpreted the latter as being due to an acoustic contribution convoluted with the H-bond bending vibrational mode, whereas the

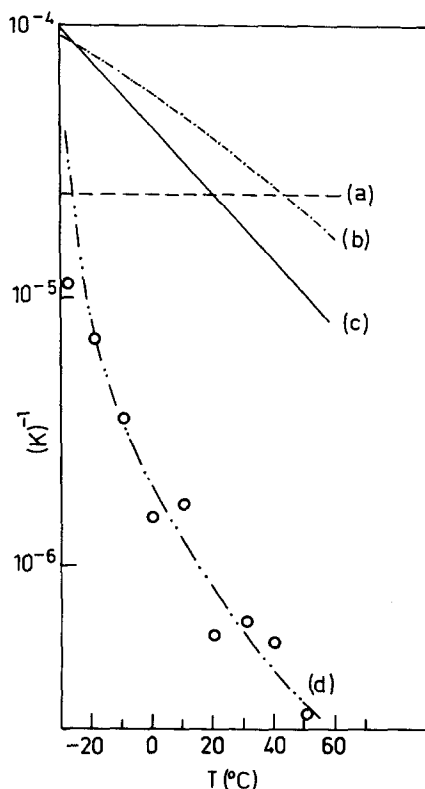


FIG. 7. Temperature evolution of: Curve (a):  $dn_x/dT$  (Ref. 43). Curve (b):  $df_4/dT$  (Ref. 48). Curve (c):  $dN_5/dT$  (Ref. 21). Curve (d):  $dI_{\text{VH}}^{\text{slow}}/dT$  (this work). Open circles:  $(\partial\rho_1/\partial T)_P$  (Ref. 23).

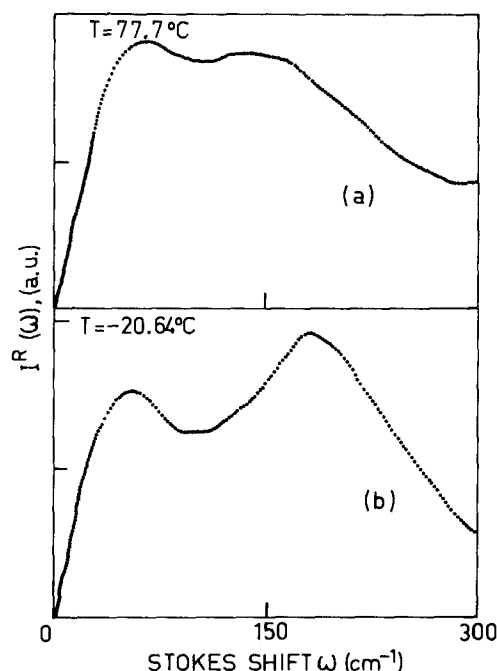


FIG. 8. Reduced depolarized Raman intensity for two temperatures. (a) Normal region; (b) supercooled region.



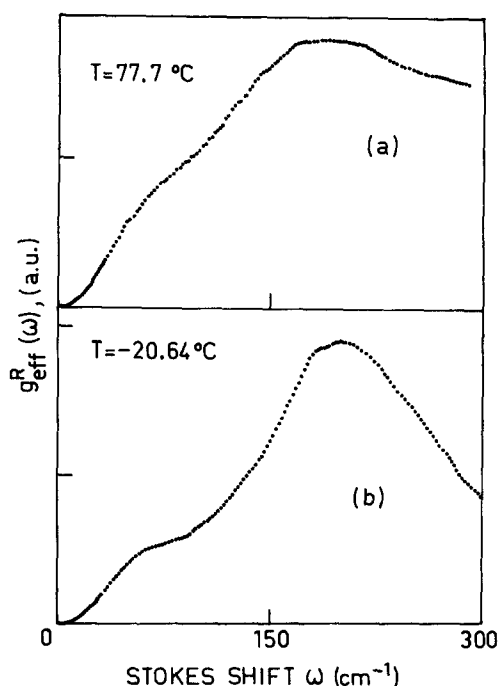


FIG. 9. Raman effective VDOS for two temperatures. (a) Normal region; (b) supercooled region.

higher frequency optical contribution is originated by the H-bond stretching mode of the  $\text{H}_2\text{O}$  molecules within the tetrahedral cage. It is to be stressed, however, that both  $I_{(\omega)}^R$  and  $g_{\text{eff}}^R(\omega)$  give all the dynamical information in our system and differ from the “true” generalized frequency distribution  $g(\omega)$  because the light scattering response gives this quantity times the function  $P(\omega)$ , as discussed elsewhere. At room temperature, by a direct comparison between a Raman scattering and an incoherent inelastic neutron scattering experiment,<sup>24</sup> we have obtained the Raman electron–vibration coupling function  $P(\omega)$  without the use of any theoretical model. The function  $P(\omega)$  is, as expected,  $\omega$  dependent. In particular, it was shown that the coupling function to the acoustic vibrations behaves like

$$(\omega/V_L)^2 \cdot \exp(-2\pi\sigma\omega/V_L)^2,$$

where  $V_L$  is the longitudinal high frequency sound velocity and  $\sigma$  is the value of a correlation length giving the spatial extent of the water structure in which the acoustic modes propagate in phase. At room temperature, this “dynamical” correlation length turns out to be 3.5 Å. Unfortunately, because the very low frequency inelastic neutron scattering measurements have not been carried so far in the supercooled phase, it is not possible to follow the temperature evolution of this parameter. Finally, it is to be noticed that the MD calculations,<sup>15</sup> give the  $\omega$  dependence of Fourier transform of the velocity–velocity time correlation function in water at room temperature. Without going into details we stress the high similarity between our  $I_{(\omega)}^R$  and the spectral density  $\tilde{z}(\omega)$  of the mass center velocity autocorrelation function, as obtained by Impey–Madden and McDonald,<sup>15</sup> the differences between them being due to the  $\omega$  dependence of the coupling function  $P(\omega)$ .

## V. CONCLUDING REMARKS

In this paper we have studied in some detail the nature of the depolarized quasielastic and inelastic light scattering spectral contribution in bulk water from the normal to the deeply supercooled liquid state. The good quality of the spectra obtained due to the high optical purity of our samples and to the careful optimization of the experimental apparatus, allowed us to perform a quantitative analysis of the Rayleigh wing and of the inelastic low frequency vibrational features. The quasielastic component shows a fine structure, and at least three symmetric contributions are detected. The intensity and linewidth of the fast and slow contributions are connected to the decay of the local order due to the center of gravity correlations, triggered by the presence of the strong intermolecular hydrogen bond. The fast central component is related to the time evolution of the extent of H bonding. We have unambiguously discovered and analyzed a slow central component, whose presence can be seen for temperatures lower than 10 °C. We have related this to the dynamical evolution of more extended structures (polyhedra), in close analogy with the results obtained by the analysis of the Landau–Placzek ratio.<sup>23</sup> The ultraslow contribution whose origin can be due to the translational diffusional motion convoluted with possible viscoelastic “transverse” contributions (at least for temperatures lower than –10 °C), is presently under examination in our laboratory. Finally a collective depolarized inelastic contribution is present, whose spectral features are detected from 0–300  $\text{cm}^{-1}$  of Stokes shift, provided all the quasielastic contributions are subtracted from the spectra. We obtained a Raman effective density of states that, in the low frequency region, seems to be a convolution of acoustical and lattice optical modes. Our results confirm conclusively that the liquid water, especially in the supercooled phase, is best understood in terms of locally ordered, dynamically correlated patches, in which the hydrogen bond plays the main role.

<sup>1</sup>C. A. Angell, in *Water: A Comprehensive Treatise*, edited by F. Franks (Plenum, New York, 1982), Vol. 7, pp. 1–81, and references therein.

<sup>2</sup>C. A. Angell, *Annu. Rev. Phys. Chem.* **34**, 593 (1983).

<sup>3</sup>J. C. Hindman, *J. Chem. Phys.* **60**, 4488 (1974).

<sup>4</sup>G. Maisano, P. Migliardo, F. Aliotta, C. Vasi, F. Wanderlingh, and G. D’Arrigo, *Phys. Rev. Lett.* **52**, 1025 (1984).

<sup>5</sup>J. Teixeira, M. C. Bellissent-Funel, S. H. Chen, and A. J. Dianoux, *J. Phys. (Paris) Colloq.* **7**, 65 (1984).

<sup>6</sup>S. Krishnamurthy, R. Bansil, and J. Wiafe-Akenten, *J. Chem. Phys.* **79**, 5863 (1983).

<sup>7</sup>Y. Yeh, J. H. Bilgram, and W. Kanzig, *J. Chem. Phys.* **77**, 2317 (1982).

<sup>8</sup>F. H. Stillinger and T. A. Weber, *J. Phys. Chem.* **87**, 2833 (1983).

<sup>9</sup>S. A. Rice and M. G. Sceats, *J. Phys. Chem.* **85**, 1108 (1981).

<sup>10</sup>H. E. Stanley, R. L. Blumberg, and A. Geiger, *Phys. Rev. B* **28**, 1626 (1983).

<sup>11</sup>H. E. Stanley, R. L. Blumberg, A. Geiger, P. Mausbach, and J. Teixeira, *J. Phys. (Paris) Colloq.* **7**, 3 (1984).

<sup>12</sup>D. C. Rapaport, *Mol. Phys.* **50**, 1151 (1983).

<sup>13</sup>F. H. Stillinger, *Science* **209**, 451 (1980).

<sup>14</sup>A. Geiger, P. Mausbach, J. Schmitker, R. L. Blumberg, and H. E. Stanley, *J. Phys. (Paris) Colloq.* **7**, 13 (1984).

<sup>15</sup>R. W. Impey, P. A. Madden, and I. R. McDonald, *Mol. Phys.* **46**, 513 (1982).

<sup>16</sup>W. L. Jorgensen, J. Chandrasekhar, J. D. Madura, R. W. Impey, and M. L. Klein, *J. Chem. Phys.* **79**, 926 (1983).



- <sup>17</sup>P. A. Kollman and L. C. Allen, *Chem. Rev.* **72**, 283 (1972).
- <sup>18</sup>A. H. Narten and H. A. Levy, in *Water: A Comprehensive Treatise*, edited by F. Franks (Plenum, New York, 1972), Vol. 1, p. 311–332.
- <sup>19</sup>J. C. Dore, *J. Phys. (Paris) Colloq.* **7**, 49 (1984).
- <sup>20</sup>See, for example, D. E. Eisenberg and W. Kauzmann, *The Structure and Properties of Water* (Oxford University, Oxford, 1969).
- <sup>21</sup>R. J. Speedy, *J. Phys. Chem.* **88**, 3364 (1984).
- <sup>22</sup>G. D'Arrigo, G. Maisano, F. Mallamace, P. Migliardo, and F. Wanderlingh, *J. Chem. Phys.* **75**, 4264 (1981).
- <sup>23</sup>G. Maisano, D. Majolino, F. Mallamace, P. Migliardo, F. Aliotta, C. Vasi, and F. Wanderlingh, *Mol. Phys.* (to be published).
- <sup>24</sup>G. Maisano, P. Migliardo, M. P. Fontana, M. C. Bellissent-Funel, and A. J. Dianoux, *J. Phys. (Paris) Colloq.* **18**, 1115 (1985).
- <sup>25</sup>M. P. Fontana, G. Maisano, P. Migliardo, M. C. Bellissent-Funel, and A. J. Dianoux, *J. Phys. (Paris)* **7**, 151 (1984).
- <sup>26</sup>G. Eckardt and W. G. Wagner, *J. Mol. Spectrosc.* **19**, 407 (1966).
- <sup>27</sup>B. J. Berne and R. Pecora, *Dynamic Light Scattering* (Wiley, New York, 1976), pp. 310–326.
- <sup>28</sup>C. J. Montrose, J. A. Bucaro, J. Marshall-Coakley, and T. A. Litovitz, *J. Chem. Phys.* **60**, 5025 (1974).
- <sup>29</sup>W. Danninger and G. Zundel, *J. Chem. Phys.* **74**, 2769 (1981).
- <sup>30</sup>F. J. Bartoli and T. A. Litovitz, *J. Chem. Phys.* **56**, 413 (1972).
- <sup>31</sup>P. A. Egelstaff, *J. Chem. Phys.* **53**, 2590 (1970).
- <sup>32</sup>F. Volino, in *Microscopic Structure and Dynamics of Liquids*, edited by J. Dupuy and A. J. Dianoux (Plenum, New York, 1977), pp. 221–300.
- <sup>33</sup>T. Keyes and D. Kivelson, *J. Chem. Phys.* **56**, 1057 (1972).
- <sup>34</sup>G. Fytas and Th. Dorfmueller, *J. Chem. Phys.* **75**, 5232 (1981).
- <sup>35</sup>R. Shuker and R. Gammon, *J. Chem. Phys.* **55**, 4784 (1971).
- <sup>36</sup>F. Aliotta, G. Maisano, N. Micali, P. Migliardo, C. Vasi, F. Wanderlingh, R. Triolo, and G. P. Smith, *J. Chem. Phys.* **76**, 3987 (1982).
- <sup>37</sup>F. Aliotta, G. Maisano, P. Migliardo, C. Vasi, and F. Wanderlingh, *J. Chem. Phys.* **75**, 613 (1981).
- <sup>38</sup>M. C. Bellissent-Funel, R. Kahn, A. J. Dianoux, M. P. Fontana, G. Maisano, P. Migliardo, and F. Wanderlingh, *Mol. Phys.* **52**, 1479 (1984).
- <sup>39</sup>O. Conde and J. Teixeira, *Mol. Phys.* **44**, 525 (1983).
- <sup>40</sup>O. Conde and J. Teixeira, *Mol. Phys.* **53**, 951 (1984).
- <sup>41</sup>R. A. McPhail and D. Kivelson, *J. Chem. Phys.* **80**, 2102 (1984).
- <sup>42</sup>B. Quentrec, *Phys. Rev. A* **15**, 1304 (1976).
- <sup>43</sup>C. A. Angell, *J. Chem. Phys.* **75**, 3698 (1971).
- <sup>44</sup>F. L. Will, *Introduction to Statistical Thermodynamics* (Addison-Wesley, Reading, MA, 1960), pp. 181–182.
- <sup>45</sup>D. Eisebrey and W. Kauzmann, *The Structure and Properties of Water* (Clarendon, Oxford, 1969).
- <sup>46</sup>G. E. Walrafen, in *Water: A Comprehensive Treatise*, edited by F. Franks (Plenum, New York, 1972), Vol. 1, pp. 151–214, and references therein.
- <sup>47</sup>G. Briganti, V. Mazzacurati, M. A. Ricci, G. Signorelli, and M. Nardone, *Solid State Commun.* **42**, 493 (1982).
- <sup>48</sup>M. E. Stanley and J. Teixeira, *J. Chem. Phys.* **73**, 3034 (1980).
- <sup>49</sup>See, for example, M. M. Brodsky, in *Light Scattering in Solids*, edited by M. Cardona (Springer, Berlin, 1975), pp. 204–251.